28 Mar 2001, 4:00 pm - 6:30 pm

Effective Stress Analysis of Pile Foundations Showing Various Damage Patterns in Liquefied Deposits During 1995 Hyogoken-Nambu Earthquake

Masanobu Miyazaki
Tokyo Institute of Technology, Japan

Sadayuki Ishizaki
Taisei Corporation, Japan

Kohji Tokimatsu
Tokyo Institute of Technology, Japan

EFFECTIVE STRESS ANALYSIS OF PILE FOUNDATIONS SHOWING VARIOUS DAMAGE PATTERNS IN LIQUEFIED DEPOSITS DURING 1995 HYOGOKEN-NAMBU EARTHQUAKE

Masanobu MIYAZAKI
Tokyo Institute of Technology
Meguro-ku, Tokyo 152-8552

Sadayuki ISHIZAKI
Taisei Corporation
Totsuka-ku, Yokohama 245-0051

Kohji TOKIMATSU
Tokyo Institute of Technology
Meguro-ku, Tokyo 152-8552

ABSTRACT

Effective stress analysis is conducted for six buildings that suffered various patterns of damage during soil liquefaction in the 1995 Hyogoken-Nambu earthquake, in order to examine major causes of the damage as well as the effectiveness of the analytical procedure. A comparison of the computed result with the filed observation indicates that the effective stress analysis is capable of discriminating damaged from undamaged foundations as well as of estimating the damage portion and severity with a reasonable degree of reliability. The analytical result also shows that: (1) the damage to pile heads is mainly due to the inertia force from the superstructure and the damage at depths below the pile head is mainly due to the kinematic force resulting from ground displacements; (2) because of their ductile behavior, steel reinforced concrete piles are immune from extensive damage; and (3) to enclose a pile foundation with diaphragm walls can reduce pile damage but can increase the response of the superstructure as well as the shear force and moment particularly in the lower levels of buildings.

INTRODUCTION

Extensive damage to pile foundations occurred due to soil liquefaction and lateral spreading in the 1995 Hyogoken-Nambu earthquake. A large number of case histories of pile foundations have been presented, based on field investigation including excavation of pile heads (e. g., Kansai Branch of Architectural Institute Japan (AIJ), 1996; AIJ et al., 1998). In addition to integrity tests for piles, several methods were used for detecting pile damage below the ground surface. Borehole camera surveys have identified damage portions and severity, and inclinometer surveys have provided data to estimate deformed shapes with depth of hollow piles.

The extensive field investigation showed that the damage portion and severity varied depending on such factors as the rigidity and ductility of the foundations, as well as the soil profile and the type of superstructure. To simulate such difference in field behavior and to evaluate stresses developed in piles, the various analysis methods including those using the Finite Element Method have been presented. It is however unclear whether those analysis methods can discriminate damaged from undamaged foundations and reasonably estimate damage portion and severity.

The object of this paper is therefore to conduct the dynamic effective stress analysis of buildings that showed various patterns of damage in the Hyogoken-Nambu earthquake and to examine the applicability of the dynamic analysis for estimating damage portion and severity.

DAMAGE FEATURES OF BUILDING AND FOUNDATION

Case histories of six buildings, hereby named as buildings A-F, that suffered various patterns of damage during soil liquefaction in the 1995 Hyogoken-Nambu earthquake are analyzed. Figure 1 shows a map showing the distribution of these buildings. They were located on reclaimed lands in Kobe City, including Port and Rokko Islands, Fukaehama, and Mikagehama where soil liquefaction extensively occurred.

The damage to pile foundations of these buildings was extensively investigated after the earthquake. Table 1 summarizes the characteristics of the buildings, pile foundations, and damage features. Building A did not show any tilt in spite of cracks in piles at two depths below the ground surface. Building B tilted largely due to shear failures near the pile head in addition to cracks near the bottom of the liquefied fill. Building C and D also tilted largely due to vital cracks of piles at depths below the pile heads. Building E did not suffer any damage to piles or to its superstructure. Building F suffered damage to its superstructure without any damage to its foundation.

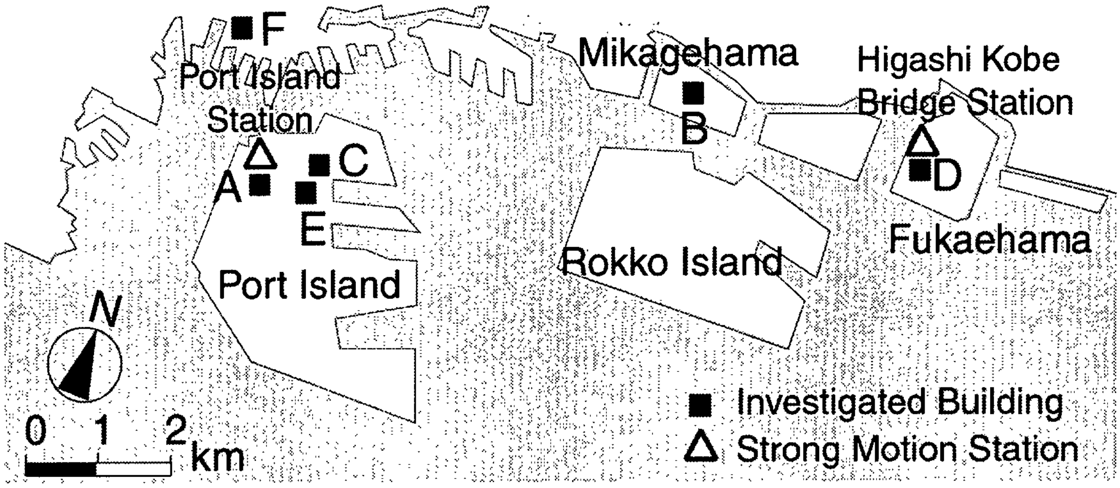

Fig. 1. Map showing distribution of building and strong motion stations

Table 1. Characteristics of pile foundations of buildings used in this study

Building or Site	Building Type [1]	No. of Story	Pile Type [3]	Pile Diameter or Wall Thickness (mm)	Foundation Damage	Building Tilt	Superstructure Damage	References
A	RC	2	PHC-A	500	Pile damage at the middle and the bottom of the liquefied fill	Non	Non	9
B	RC	4	PHC-A	350	Pile damage at the pile haad (shear failure) and the bottom of the liquefied fill	1/68	Non	8
C	RC	2	PHC-A	450	Pile damage at 3 m depth (near the ground water table) and the bottom of the liquefied fill	1/30	Non	7
D	RC	5	SC+PHC-A	600	Pile damage at the bottom of the liquefied fill	1/29	Non	5
E	RC	4	SC+PHC-B	500	Non	Non	Non	3
F	SRC	11 + 2 [2]	CC+ diaphagm walls	1500(Pile)+ 600(Wall)	Non	Non	Damage due to inertia force	2

1) RC: Reinforced concrete, SRC: Steel framed reinforced concrete 2) Basement
3) PHC: Prestressed high strength concrete pile, SC: Steel reinforced concrete pile, CC: Cast-in-place concrete pile

ANALYSIS METHOD

Two-dimensional effective stress response analysis based on the Finite Element Method (Iai et al., 1992) was modified and used. In the analysis, in addition to the soil elements, both the piles and superstructure were assumed to be nonlinear. The interaction between the soil and pile was modeled using a nonlinear p-y spring. The initial modulus and the maximum resistance of the p-y spring were scaled in accordance with the pore water pressure developed near the pile.

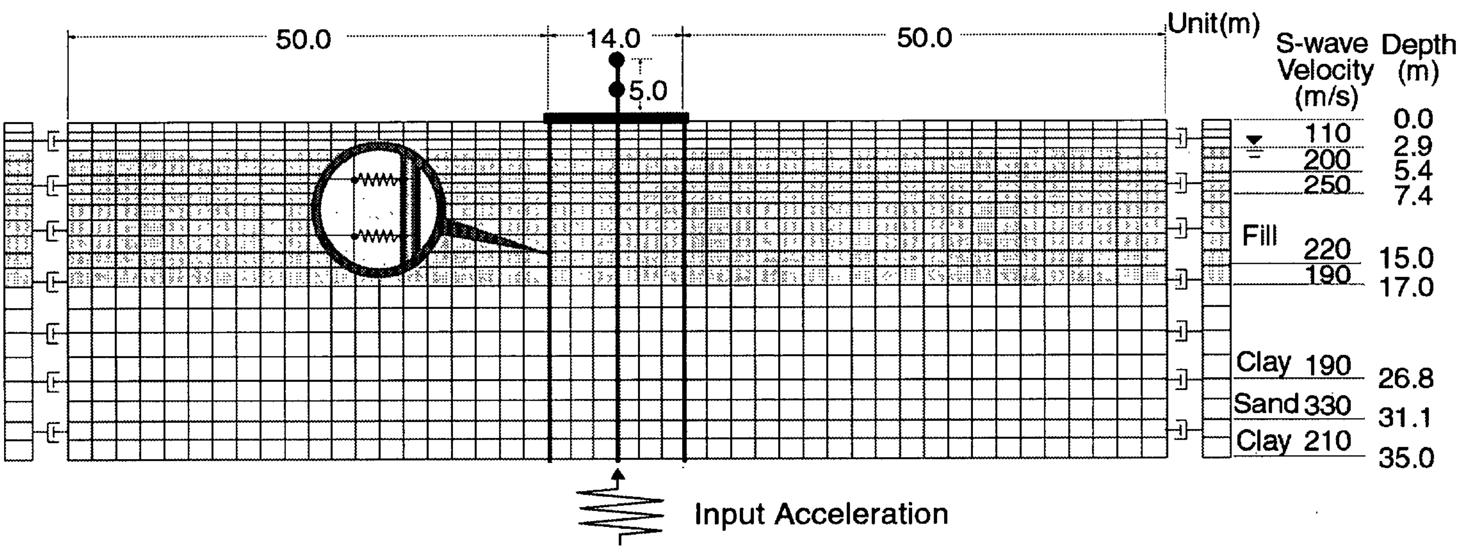

Fig. 2. Analytical model of Building A

Figure 2 shows the analytical model for Building A. Viscous boundaries were used at both sides and the fixed boundaries at the bottom. The effects of both in-plane and out-of-plane walls were considered for Building F. An N-S component of the downhole strong motion record obtained in the Kobe area during 1995 Hyogoken-Nambu earthquake was used as an input motion to the base of each analytical model. The record at 32 m depth of the Kobe Port Island station was used for Buildings A, C, and E; and the record at 83 m depth of the same site for Building F. The record at 33m depth of the Higashi Kobe Bridge station was used for Buildings B and D.

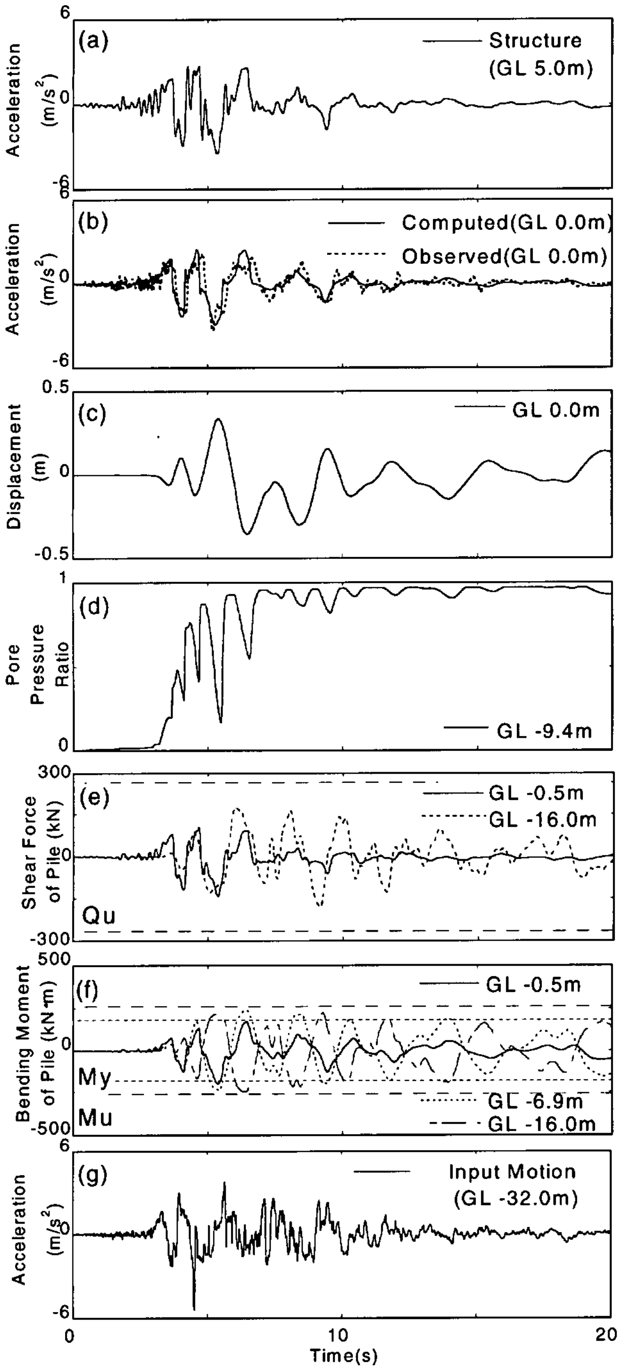

Fig. 3. Selected time histories of analytical result at Building A

ANALYTICAL RESULTS

Figure 3 shows the computed time histories of acceleration, displacement, pore water pressure ratio, and shear force and bending moment in pile at selected depths, as well as the input acceleration for Building A. In the figure, Qu is ultimate value of shear force, My is bending moment at yielding of tension bars of PHC piles or of steel at extreme tension fiber of SC piles, and Mu is bending moment at concrete crashing at extreme compression fiber of PHC and SC piles.

In Fig. 3(b), the ground surface acceleration observed at the Port Island station is also shown with a broken line for comparison. The computed acceleration shows a good agreement with the observed record, indicating that the analysis has been done properly. Within 3-5 s after the initiation of the shaking, the pore water pressure in the fill rises rapidly accompanied by large ground displacement, suggesting that soil liquefaction occurred in 5-7 s. After the development of the pore pressure, the amplitude of the ground surface acceleration decreases, while that of the ground surface displacement maintains a large value.

Both shear force and bending moment at the pile head that take large values at the early stage of shaking, decrease significantly after 7 s when the reclaimed fill liquefies completely. The trend is very similar to that of the superstructure acceleration shown in Fig. 3(a). In contrast, the shear force at the bottom of the liquefaction layer, i.e., 16m depth, oscillates largely even after liquefaction, the trend of which is very similar to that of the ground displacement shown in Fig. 3(c). The time histories of the bending moment at 6.9 and 16 m depths also follow the trend of the ground surface displacement. The above similarities suggest that the inertia force from the superstructure governs the stress near the pile head, and the ground displacement controls the stresses at depths below the pile head.

The distributions of the computed maximum shear force and bending moment for Building A are shown in Figure 4 with solid lines. Also shown in the figure are the detected cracks in pile and a boring log of the site. The computed maximum shear force is less than Qu at any depth. The maximum bending moment, in contrast, exceeds My within the liquefied fill, and becomes close to Mu near the depth of 7.0 m and at the bottom of liquefied fill where cracks concentrated as shown in Fig. 4(c).

The relationship between bending moment and curvature for the pile of Building A is shown with a solid line in Fig. 4(e), in which ϕ_c and ϕ_u are the curvatures at concrete failure at tensile edge and at concrete crashing at compression edge, respectively. Also shown in the figure with a solid line and triangles are the relation assumed in the analysis and the maximum computed curvatures, ϕ_{max}, at critical depths.

The maximum curvature is very close to ϕ_c at the pile head where minute cracks were reported from field investigation. Both the maximum curvatures at the 6 and 16 m depths, in contrast, are larger than ϕ_c but far less than ϕ_u. Field investigation, nevertheless, showed that vital horizontal cracks occurred with cutoff of reinforcing bars at those depths. Probably, the large curvatures that repeatedly occurred during shaking induced tensile cracks around the pile. This in turns caused significant reduction in the shear strength of the pile, leading to the cutoff of reinforcing bars. The computed results therefore appear to simulate the damage features of the piles.

To evaluate the effect of ground displacement on pile damage, the analysis is also conducted on a model without the superstructure for Building A. The computed results are shown with broken lines in Figs. 4(a) and (b). When the superstructure is removed, both maximum shear force and bending moment at the pile head decrease significantly, while their values at depths below 3 m are unchanged. This confirms the previous statement that the inertia force from the superstructure governs the stress near the pile head, and the ground displacement controls the stresses at depths below the pile head.

The distributions of the computed maximum shear force and bending moment for Buildings B-E are shown in Figures 5-8. Also shown in each figure are the detected cracks in thpile, and a boring log of the site. The maximum shear force is close to Qu only near the pile head of Building B, while it is far below Qu at other buildings. The maximum bending moment is also close to Mu at the pile head of Building B, indicating that bending shear failure could occur near the pile head. This is consistent with the field observation in which only the pile head of Building B suffered bending shear failure.

The maximum bending moment of Building B is close to Mu at the bottom of liquefied fill and that of Building C is close to Mu at two depths below the ground surface. The depths at which the maximum bending moment occurs correspond to the place where vital cracks were observed. The moment-curvature relations for the piles of Building B and C as well as the computed ϕ_{max} at critical depths are shown in Figs. 5(e) and 6(e). The maximum curvatures at the critical depths of both buildings are larger than ϕ_c but less than ϕ_u. This again suggests that tensile cracks around the piles might have been a major cause leading to the vital damage. The FEM analysis for Building B and C therefore appears capable of detecting damage portions and failure modes.

Figure 7(b) shows that the maximum bending moment of Building D is very close to Mu at the pile head and the bottom of the liquefied fill. The maximum bending moment of Building E is also close to Mu at the pile head, but far less than Mu at the bottom of the liquefied fill, as shown in Figure 8(b). It seems unclear whether the analysis method is capable

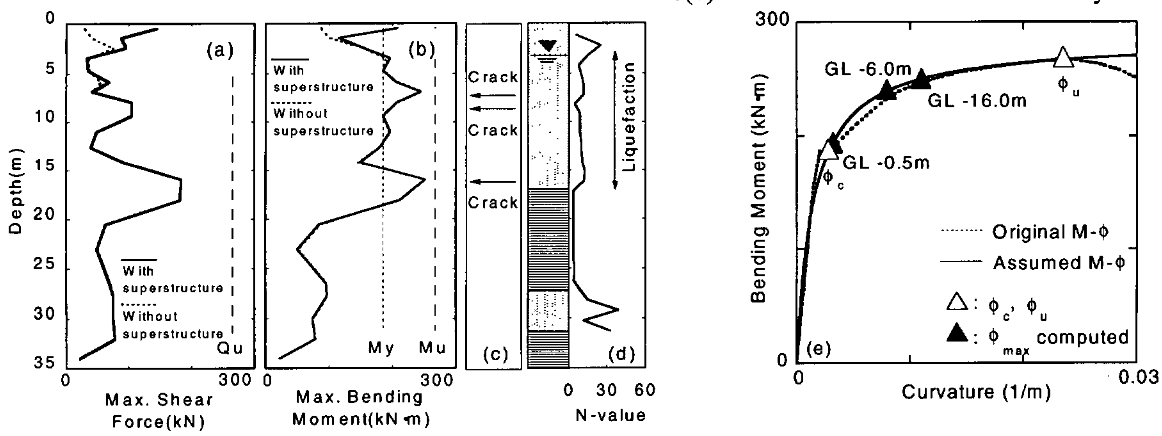

Fig. 4. Computed maximum shear force and bending moment, pile damage, boring log and moment-curvature relation for Building A

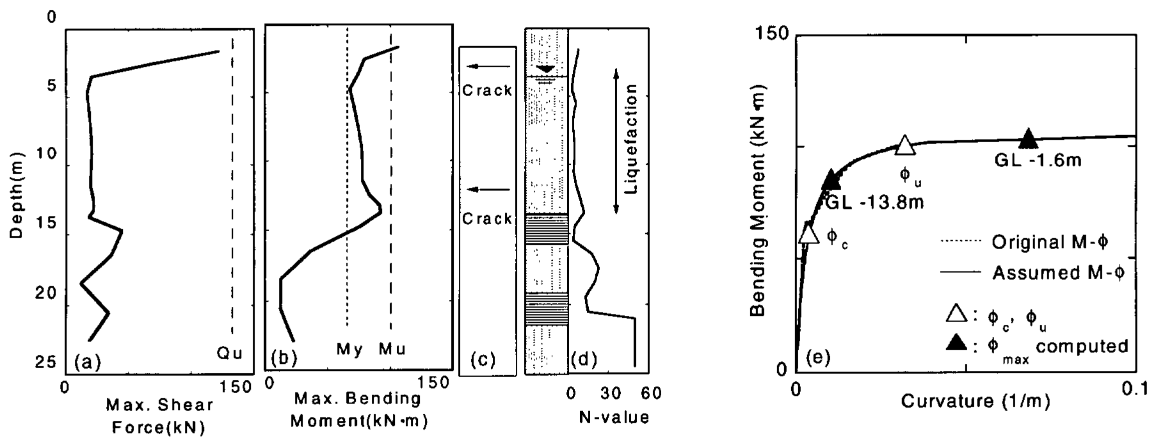

Fig. 5. Computed maximum shear force and bending moment, pile damage, boring log and moment-curvature relation for Building B

of predicting the difference in damage between the two buildings. Thus, the moment-curvature relations at critical depths of the two buildings are compared in Figures 9 and 10. Figure 9 shows that, although the bending moments at the pile head of both buildings are close to Mu, the maximum curvature at Building E is far less than ϕ_u. This is consistent with the field observation in which no damage was detected at the pile head of Building E. The computed result for Building D, in contrast, appears inconsistent with the field observation in which any vital damage was not detected near the pile heads. Probably because of their ductile nature, the steel reinforced concrete piles were immune from extensive damage.

At the bottom of the liquefied layer, the maximum curvature is far less than ϕ_u at Building E but it exceeds ϕ_u at Building D. The large curvature at Building D might have caused the vital damage to piles, leading to its large tilt. The computed results therefore appear consistent with the field observation, suggesting that the analysis can differentiate damaged from undamaged foundations with a reasonable degree of accuracy.

Figures 11 and 12 show the distributions of computed maximum shear force and bending moment in the pile and those of computed maximum shear force and acceleration in the superstructure of Building F.

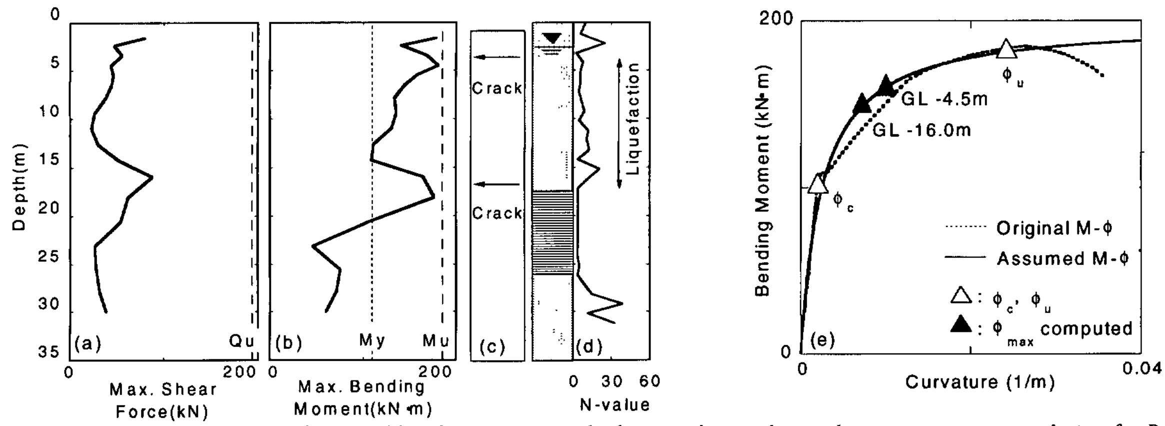

Fig. 6. Computed maximum shear force and bending moment, pile damage, boring log and moment-curvature relation for Building C

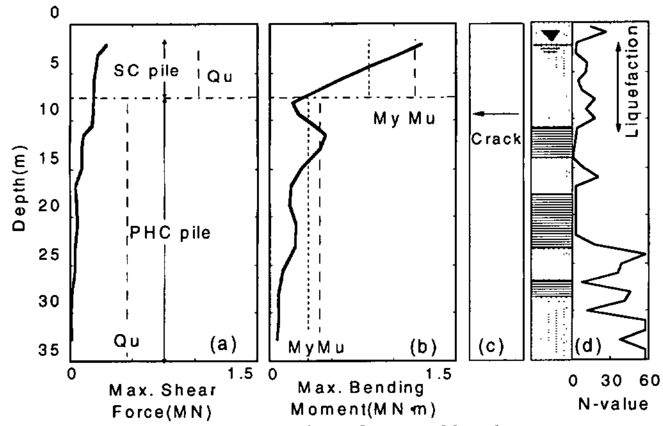

Fig. 7. Computed maximum shear force and bending moment, pile damage, and boring log for Building D

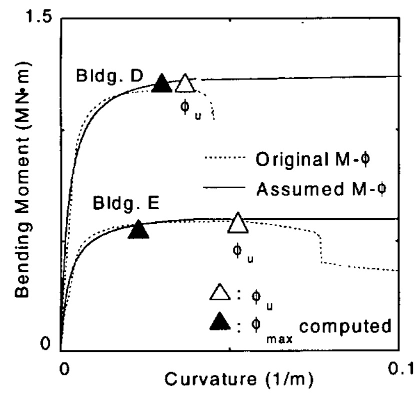

Fig. 9. Relation between bending moment and curvature at pile heads for Buildings D and E

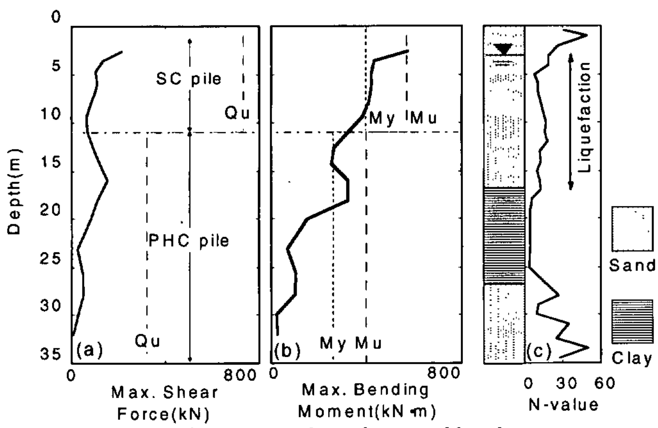

Fig. 8. Computed maximum shear force and bending moment, pile damage, and boring log for Building E

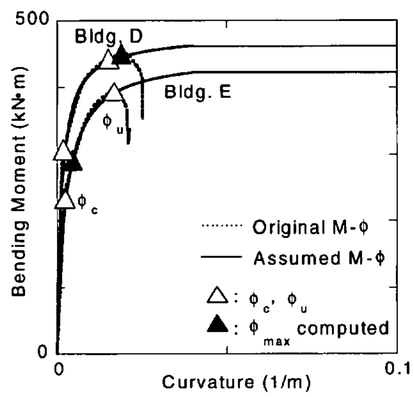

Fig. 10. Relation between bending moment and curvature at bottom of liquefied fill for Buildings D and E

Both the maximum shear force and bending moment are far below the ultimate values, being consistent with the field observation in which no damage to pile was detected.

In order to confirm the effects of the diaphragm walls, the analysis was also made with a model without the diaphragm walls. The computed results are shown with broken lines in Figs. 11 and 12 for comparison. When the diaphragm walls are removed, the maximum shear force and bending moment become close to the ultimate values at the pile head as shown in Fig. 11, suggesting possible damage to the foundation. This means that the diaphragm walls were effective in reducing stresses and thus eliminating possible failures near the pile heads.

When the diaphragm walls are used, however, the maximum acceleration and shear force developed in the superstructure get larger as shown in Fig. 12. Particularly, the shear force acting on the lower levels is significantly higher in the building with diaphragm walls than without them. This is one of the major factors causing the damage to superstructure of this building. It is conceivable therefore that the adoption of diaphragm walls not only has a positive effect on the foundation but also has an adverse effect on the superstructure. Such effects must be considered appropriately in the design of building in liquefiable soils.

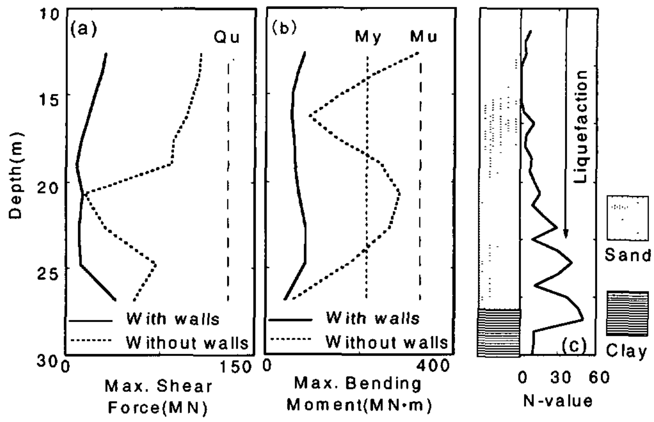

Fig. 11. Computed maximum shear force and bending moment, and boring log for Building F

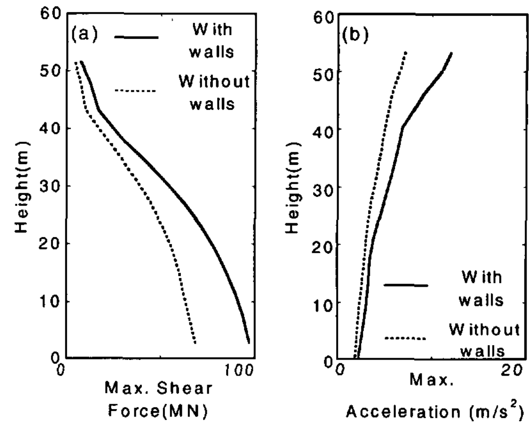

Fig. 12. Computed maximum shear force and acceleration for Building F

CONCLUSIONS

Dynamic effective stress analysis was conducted on six buildings that suffered various patterns of damage during the 1995 Hyogoken-Nambu earthquake. Based on the comparison between the observed behavior and computed result, the following conclusions can be made:

(1) The damage to pile heads is mainly due to inertia forces from superstructure and the damage at depths below the pile heads is mainly due to kinematic forces from ground displacements.
(2) Steel reinforced concrete piles are immune from extensive damage, because of their ductile behavior.
(3) To strengthen foundations with diaphragm walls is effective in reducing damage caused by ground displacements during soil liquefaction, but can increase the acceleration response of the superstructures as well as the shear stresses particularly in the lower levels of buildings.
(4) The computed results are consistent with the observed results, indicating that the analysis method used in this paper is capable of differentiating damaged from undamaged foundations and of estimating the damage portion and severity with a reasonable degree of reliability.

REFERENCES

1) Architectual Institure of Japan et al. [1988]. "Report on the Hanshin-Awaji earthquake disaster", Building Series Volume 4, Wooden Structure and Building Foundations (in Japanese).
2) BTL Committee [1998]. "Research Report on liquefaction and lateral spreading in the Hyogoken-Nambu earthquake" (in Japanese).
3) Fujii, S., Cubrinovski, M., Hyashi, T., Shimazu, S., and Tokimatsu, K. [1996]. "Response analysis of buildings with a pile foundation on a liquefied ground", Proc., 31st Japan National Conf. on Geotech. Engrg., Vol. 1, pp. 1139-1140 (in Japanese).
4) Iai, S., Matsunaga, Y., and Kameoka, T.[1992]. "Analysis of undrained cyclic behavior of sand under anisotropic consolidation", Soil and Foundations, Vol. 32, No. 2, pp.16-20.
5) Isemoto, N., Kaneko, O., Sato, Y., Arai, T., Fujiwara, T., and Shirinashihama, S. [1998]. "Analytical studies on pile foundations damaged by soil liquefaction during the Hyogoken-nanbu earthquake", Proc., 33rd Japan National Conf. on Geotech. Engrg., Vol. 1, pp. 801-802 (in Japanese).
6) Kansai Branch of Architectural Institute of Japan [1996]. "Report on case histories of damage to building doundations in Hyogoken-Nambu earthquake", Report presented by Committee on Damage to Building Foundations, 400pp. (in Japanese).
7) Onishi, K., Namba, S., Sento, N., Horii, K., Tatsumi, Y., and Oh-oka, H. [1997]. "Investigation of failure and deformation modes of piles throughout overall length", Tsuchi to Kiso, Vol. 45, No. 3, pp. 24-26 (in Japanese).
8) Shamoto, Y., Sato, M., Futaki, M., and Shimazu, S. [1996]. "Site investigation of post-liquefaction lateral displacement of pile foundation in reclaimed land", Tsuchi to Kiso, Vol. 44, No. 3, pp. 25-27 (in Japanese).
9) Tachikawa, H., Fujii, S., Onishi, K., Suzuki, Y., Isemoto, N., and Shirahama, M. [1998]. "Investigation and analysis of pile foundation located on Kobe Port Island", Proc., 33rd Japan National Conf. on Geotech. Engrg., Vol. 1, pp. 811-812 (in Japanese).